Journal of Solid Mechanics Vol. 14, No. 2 (2022) pp. 118-130
DOI: 10.22034/jsm.2020.1904760.1623

On Validity of Analytical Method in Cracked Column Post-Buckling Analysis Using Empirical and Numerical Investigations

K. Salmalian [1], A. Alijani [1,*], H. Ramezannejad Azarboni [2]

[1]*Department of Mechanical Engineering, Bandar Anzali Branch, Islamic Azad University, Bandar Anzali, Iran*
[2]*Department of Mechanical Engineering, Ramsar Branch, Islamic Azad University, Ramsar, Iran*

Received 18 January 2022; accepted 23 March 2022

ABSTRACT

The three analytical, finite element and experimental methods are applied to study the nonlinear buckling of cracked columns. The original aim of this research is to investigate the validity of the common analytical method in an analogy with the experimental method and the finite element method of MATLAB programming-based. The literature review shows that papers applied this analytical method without considering its drawbacks to determine the post-buckling results. Results in the linear part of the analytical method are in close accordance with the two others, while a clear difference in the nonlinear part of the analytical method is observed with the actual results obtained from the experimental tests and numerical results of the finite element method. An in-depth discussion is represented to find out the main reasons of this difference. The conversion matrix technique in the finite element method and dividing the column into two segments in the analytical method are used to include the crack parameters in relations according to the continuity conditions in the crack tip. An investigation is performed to study the effect of the crack depth and position on the critical buckling load and the post-buckling path.

Keywords : Analytical method; Cracked column; Experimental method; Nonlinear buckling; Finite element method.

1 INTRODUCTION

MANY different methods are used to evaluate the crack effect in structures. Accuracy, capability, flexibility, and solution cost are the main parameters to select or to reject a method for the analysis. The analytical method in the subject of the cracked structure is implemented based on the energy release rate parameter in which the crack is modeled using Dirac's delta function or the rotational spring [1-9]. Another reliable method in the analysis of the cracked structures is the numerical method. FEM, XFEM and Meshless methods are generally considered in the category of the numerical method. Alijani et al. [10, 11] used FEM to investigate the nonlinear

*Corresponding author. Tel.: +98 911 1351067; Fax.: +98 133 3730223.
E-mail address: alijani@iaubanz.ac.ir (A.Alijani)

deflection, natural frequency, and stress intensity factor of the cracked beam. A comparison between FEM and XFEM in the modeling of the cracked structures can be seen in [12]. Moreover, various research works in the framework of XFEM and Meshfree methods can be found for the analysis of cracked structures in [14-15]. Empirical tests are a convenient way to validate the results of analytical and numerical methods. Some experimental investigations on the cracked structures can be seen in [15-18]. On the other side, many research works have been specifically published to investigate linear and nonlinear buckling analysis of cracked columns using analytical, numerical and experimental methods. The initial crack in columns has a destructive effect on the strength and stability. Accordingly, the investigation of the buckling and post-buckling behavior of cracked columns has a considerable significance. Anifantis and Dimarogonas [19] and [20] used the analytical method to study the post-buckling behavior of perfect and imperfect columns with a transverse crack surface considering the local flexibility. Ke et al. [21] also applied the analytical method in post-buckling and vibration analysis of the cracked functionally graded Timoshenko beams. 3D finite element method was employed to study the effect of the crack surfaces contact on the post-buckling behavior of the cracked column in [22]. Akbas and et al. [23-25] utilized the finite element method to evaluate the post-buckling behavior of cracked columns made of isotropic, composite and functionally graded materials. Yang and Bradford presented a solution based on the method of the minimum total potential to investigate the buckling and post-buckling behavior of weakened columns under thermal loading [26]. Many research works about post-buckling analysis of cracked columns have been published [27-30] in which different subjects including delamination, shear effect, cracked plates, and FG materials were discussed. Moreover, the buckling behavior of intact columns can be seen in many research works, e.g. [31-40].

The main discussion in this research is to verify the analytical method in the post-buckling analysis of intact and cracked columns represented in [19, 20, 31, 33, 34, 38]. Therefore, a comprehensive investigation is performed to recognize the technical ability of the common analytical method in the nonlinear buckling analysis. The two experimental and FE methods are used to validate the analytical method. Unexpected results of the analytical method caused a meaningful comparison with the two other methods is made. A check on the mathematical relations and the solution process is carried out to identify reasons of the difference in the analytical method. Because of the close accordance of the empirical results with FEM results, it is applied as a reliable method to study the effect of the crack on the critical buckling load and post-buckling results.

2 CRACK MODELLING

Fig. 1(a) illustrates a uniform Euler-Bernoulli column including an edge crack under the compressive axial load. The crack shown in Fig. 1(a) is modeled by a massless rotational spring. Fig. 1(b) shows the rotational spring whose flexibility is denoted by ψ that is inversely related to the stiffness of rotational spring, k_{ds} .

(a) (b)

Fig.1
Geometrical representation. a) Euler-Bernoulli column including edge crack; b) Crack modelling via rotational spring.

Yokoyama and Chen [4] proposed a formula between the stress concentration factor and the spring stiffness in problems that the bending moment is applied to the structure as [4]:

$$K_I = \frac{6M}{bh^2}\sqrt{(\pi a)}F_M(\xi) \quad \text{for } 0 \le \xi \le 0.6\,,\ \xi = \frac{a}{h}\,, \quad K_I = \frac{3.99M}{bh\sqrt{h}\sqrt{(1-\xi)^3}} \quad \text{for } 0.6 \le \xi \le 1$$

$$F_M(\xi) = \sqrt{\left(\frac{2}{\pi\xi}\right)tan\frac{\pi\xi}{2}}\,\frac{0.923 + 0.199\left[1-\sin\left(\frac{\pi\xi}{2}\right)\right]^4}{\cos\left(\frac{\pi\xi}{2}\right)} \tag{1}$$

The stiffness factor of the corresponding spring, k_{ds} , is computed as follows:

$$\frac{1}{k_{ds}} = \frac{2b\left(1-\nu^2\right)}{E}\int_0^{\bar{a}}\left(\frac{K_I}{M}\right)^2 da \tag{2}$$

Fig. 2 shows the effective parameters of the analysis around the crack area in which the continuity conditions at the crack point are defined according to Eq. (3),[11].

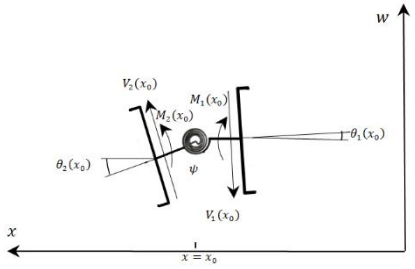

Fig.2
Displacements, slops, bending moments and shear forces in both sides of rotational spring.

$$\begin{aligned}
&w_1\left(x_0\right) = w_2\left(x_0\right)\\
&w_1''\left(x_0\right) = w_2''\left(x_0\right)\\
&w_1'''\left(x_0\right) = w_2'''\left(x_0\right)\\
&w_1'\left(x_0\right) - w_2'\left(x_0\right) = \psi w_1''\left(x_0\right)
\end{aligned} \tag{3}$$

In which $\psi = \frac{EI}{k_{ds}}$. As shown in Fig. 2, the crack modelling leads to divide the column into two separated segments and the rotational spring. The relations of the displacement, slope, bending moment, and shear force for the Euler-Bernoulli column under compressive force *P* are given as [41]:

$$\begin{aligned}
&\theta_1\left(x\right) = \frac{dw_1}{dx}\\
&M_1\left(x\right) = -EI\,\frac{d^2w_1}{dx^2}\\
&V_1\left(x\right) = \frac{dM_1}{dx} - P\,\frac{dw_1}{dx}
\end{aligned} \tag{4}$$

3 ANALYTICAL SOLUTION OF POST-BUCKLING OF CRACKED COLUMN

The nonlinear buckling equation for an intact column is [33]

$$w'''' + \frac{P}{EI}w'' - \frac{bh}{2}w''w'^2 = 0 \tag{5}$$

In which $k^2 = P/EI$ is called the critical buckling load parameter. The general solution of Eq. (5) for two segments of column is as follows:

$$w_1\left(x\right) = A_1 + A_2x + A_3\sin\left(kx\right) + A_4\cos\left(kx\right) \tag{6a}$$

$$w_2(x) = A_5 + A_6 x + A_7 \sin(kx) + A_8 \cos(kx) \tag{6b}$$

Here, parameters A_i are considered as constant coefficients.

3.1 Linear buckling solution

A linear differential equation of the buckling analysis can be obtained by neglecting the nonlinear term of Eq. (5), which can be used to determine the critical buckling load of the cracked column. Gurel and Kisa [41] applied a technique to solve the linear differential equation of the cracked column which yields following equations for two SS-SS and C-C boundary conditions, respectively.

$$\sin(k_c L) - \psi k_c \sin(\beta k_c L) \sin\left[(1-\beta) k_c L\right] = 0 \tag{7a}$$

$$4\sin\left(\frac{k_c L}{2}\right)\left[\sin\left(\frac{k_c L}{2}\right) - \left(\frac{k_c L}{2}\right)\cos\left(\frac{k_c L}{2}\right) + \psi k_c \left\{\sin(k_c L) - (k_c L)\cos(\beta k_c L)\cos\left[(1-\beta) k_c L\right]\right\} = 0 \tag{7b}$$

In which $\beta = X_0 / L$ and the critical buckling load parameter, k_c, can be computed using the root finding algorithm such as Newton-Raphson technique. It is clear that if $\psi = 0$ is considered, the corresponding critical buckling load parameter is determined for the intact column.

3.2 Post-buckling solution

A post-buckling analysis can be performed by computing the undefined coefficients, A_i, mentioned in Eq. (6). These coefficients are computed by considering the boundary conditions, continuity relations at the crack point, and the nonlinear differential equation. Two SS-SS and C-C boundary conditions are considered in the derivation of relations. Table 1 shows end constraints of two boundary conditions.

Table 1
Boundary conditions.

SS-SS	$w_1(0) = 0$	$\frac{d^2 w_1(0)}{dx^2} = 0$	$w_2(L) = 0$	$\frac{d^2 w_2(L)}{dx^2} = 0$
C-C	$w_1(0) = 0$	$w_1'(0) = 0$	$w_2(L) = 0$	$w_2'(L) = 0$

Four equations for each type of boundary conditions in combination with four continuity conditions of the crack point Eq. (3) give an algebraic equation system as follows:

For SS-SS end conditions

$$\begin{bmatrix} 1 & 0 & 0 & 1 & 0 & 0 & 0 & 0 \\ 0 & 0 & 0 & 1 & 0 & 0 & 0 & 0 \\ 0 & 0 & 0 & 0 & 1 & L & S_L & b \\ 0 & 0 & 0 & 0 & 0 & 0 & k^2 S_L & k^2 C_L \\ 1 & x_0 & S_{x0} & C_{x0} & -1 & -x_0 & -S_{x0} & -C_{x0} \\ 0 & 1 & kC_{x0} & -kS_{x0} & 0 & -1 & -kC_{x0} & kS_{x0} \\ 0 & 0 & -k^2 S_{x0} & -k^2 C_{x0} & 0 & 0 & k^2 S_{x0} & k^2 C_{x0} \\ 0 & -P & (EIk^3 - Pk) C_{x0} & (Pk - EIk^3) S_{x0} & 0 & P & (Pk - EIk^3) C_{x0} & (EIk^3 - Pk) S_{x0} \end{bmatrix} \begin{Bmatrix} A_1 \\ A_2 \\ A_3 \\ A_4 \\ A_5 \\ A_6 \\ A_7 \\ A_8 \end{Bmatrix} = \begin{Bmatrix} 0 \\ 0 \\ 0 \\ 0 \\ 0 \\ \frac{M}{k_{ds}} \\ 0 \\ 0 \end{Bmatrix} \tag{8}$$

For C-C end conditions

$$\begin{bmatrix} 1 & 0 & 0 & 1 & 0 & 0 & 0 & 0 \\ 0 & 1 & k & 0 & 0 & 0 & 0 & 0 \\ 0 & 0 & 0 & 0 & 1 & L & S_L & C_L \\ 0 & 0 & 0 & 0 & 0 & 1 & kC_L & -kS_L \\ 1 & x_0 & S_{x0} & C_{x0} & -1 & -x_0 & -S_{x0} & -C_{x0} \\ 0 & 1 & kC_{x0} & -kS_{x0} & 0 & -1 & -kC_{x0} & kS_{x0} \\ 0 & 0 & -k^2S_{x0} & -k^2C_{x0} & 0 & 0 & k^2S_{x0} & k^2C_{x0} \\ 0 & -P & (EIk^3-Pk)C_{x0} & (Pk-EIk^3)S_{x0} & 0 & P & (Pk-EIk^3)C_{x0} & (EIk^3-Pk)S_{x0} \end{bmatrix} \begin{Bmatrix} A_1 \\ A_2 \\ A_3 \\ A_4 \\ A_5 \\ A_6 \\ A_7 \\ A_8 \end{Bmatrix} = \begin{Bmatrix} 0 \\ 0 \\ 0 \\ 0 \\ 0 \\ \dfrac{M}{k_{ds}} \\ 0 \\ 0 \end{Bmatrix} \tag{9}$$

where S_L , C_L , S_{x0} and C_{x0} can be found in Eq.(A.3) of Appendix A.

The determination of nonzero values of coefficients, A_i , requires that the determinant of the coefficients matrix is set equal to zero. So, a non-trivial solution is found when the coefficients are expressed in terms of one coefficient, like A_2, by neglecting an arbitrary row of the equation system. In other words, the unknown coefficient A_2 in terms of the incremental axial compressive force P is determined by the integral form of the nonlinear buckling equation as follows:

$$\int_0^L \left(-k_c^2 - \frac{P}{EI} - \frac{bh}{2I} w'^2 \right) dx = 0 \tag{10}$$

Eq. (10) is an integral form of Eq. (5) by considering $w'''' = -k_c^2 w''$ while w'' is nonzero. Eqs. (A.1) and (A.2) in Appendix A represent relations in which coefficients A_i are expressed in terms of A_2, for SS-SS and C-C boundary conditions, respectively. By inserting the first derivative of displacement equation into Eq. (10), the final form of governing equation is given

$$-k^2 - \frac{P}{EI} - \frac{1}{L}\frac{bh}{2I}\left(\int_0^{x_c} w_1'^2 dx + \int_{x_c}^{L} w_2'^2 dx\right) = 0 \tag{11}$$

which gives A_2 in terms of the incremental load P. Therefore, the maximum lateral displacement for each load level and also the nonlinear load-displacement curve are determined by replacing A_i 's in Eq.(6) as follows:

$$w_1(x_0) = A_1 + A_2 x_0 + A_3 \sin(kx_0) + A_4 \cos(kx_0) \tag{12}$$

4 FEM FOR POST-BUCKLING ANALYSIS OF CRACKED COLUMN

The discretization of the column in the FEM analysis is performed using the one-dimensional element in which the nodal displacements are interpolated by cubical Hermite functions. The secant and tangent stiffness matrices are derived by including constitutive and kinematic relations into to the energy formula. The mathematical modeling of the cracked element is the key part of the analysis in the cracked column. The cracked element in FEM is discretized to three sub-elements as shown in Fig.3. Those are connected to each other through continuity conditions mentioned in Eq.(3). So, the stiffness matrices of cracked element are enriched by using crack characteristics and continuity conditions

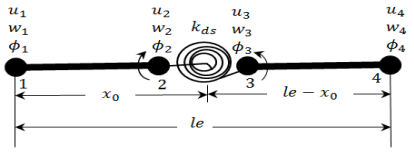

Fig.3
Cracked element.

The conversion matrix technique [2] is applied based on the transformation of the middle nodes displacements (nodes 2 and 3) to the main nodes of 1 and 4. For this reason, two converting matrices, $\boldsymbol{C}_L$ and $\boldsymbol{C}_R$ are constructed to obtain enriched stiffness matrices.

The process of the determination of enriched total stiffness matrices of the cracked column used in the presented MATLAB programming is as follows:

a) Discretization of column using 1D-element
b) Detection of the element including the crack
c) Computation of the tangent ($\boldsymbol{k}_T$) and secant ($\boldsymbol{k}_S$) matrices for intact elements [42]
d) Using the conversion technique for the cracked element represented in Appendix B.
e) Computation of the enriched tangent ($\boldsymbol{k}_{TC}$) and secant ($\boldsymbol{k}_{SC}$) stiffness matrices for the cracked element
f) Computation of the total tangent ($\boldsymbol{K}_T$) and secant ($\boldsymbol{k}_S$) stiffness matrices for the column

Moreover, the algorithm of the post-buckling analysis used in the MATLAB programming can be decomposed according to the following steps:

Initials values: $\lambda = \bar{\lambda}$ (load level), $\vec{u}_0$: initial known state

Iteration loop: $i = 0,1,\ldots$ until convergence

1. Compute $\boldsymbol{K}_T\left(\vec{u}_i\right)$, $\boldsymbol{K}_S\left(\vec{u}_i\right)$, $\vec{R}\left(\vec{u}_i\right)$
2. $\begin{cases} if\ \det\left(\boldsymbol{K}_T\left(\vec{u}_i\right)\right) < 0 \quad for\ the\ first\ negative\ \text{determinant} \\ compute\ the\ neighboring\ \text{point}: u_i = u_i + \zeta\varnothing \\ update\ \boldsymbol{K}_T\left(\vec{u}_i\right), \boldsymbol{K}_S\left(\vec{u}_i\right), \overrightarrow{R}\left(\vec{u}_i\right) \\ end \end{cases}$
3. Compute the displacement increment: $\boldsymbol{K}_T\left(\vec{u}_i\right)\overrightarrow{\Delta u}_{i+1} = \bar{\lambda}\vec{F} - \overrightarrow{R}\left(\vec{u}_i\right)$
4. Compute the updated displacement: $\vec{u}_{i+1} = \vec{u}_i + \overrightarrow{\Delta u}_{i+1}$.
5. Convergence test
6. $\bar{\lambda}\vec{F} - \overrightarrow{R}\left(\vec{u}_i\right)\begin{cases} \leq \varepsilon \rightarrow set\ \vec{u}_{k+1} = \vec{u}_{i+1}\ Go\ to\ next\ load\ level \\ \geq \varepsilon \rightarrow set \qquad\qquad i = i+1 \end{cases}$

In which $\vec{R} = \boldsymbol{K}_S\left(\vec{u}_i\right)\vec{u}_i$ and ζ and $\varnothing$ are the perturbation factor and the eigenvector associated to the minimum eigenvalue, respectively.

The tangent stiffness matrix and the internal force vector $\vec{R}$ are firstly determined in terms of the already known displacement vector. The determinant of tangent stiffness matrix is computed based on the decomposition process of this matrix in each load step. Then the perturbation at the critical point is applied to find the neighboring point for a successful switch to the post-buckling path.

5 RESULTS AND DISCUSSION

The results of the nonlinear buckling analysis in perfect and cracked columns are reported based on three experimental, analytical and numerical methods. 63-*cm*-long columns made of steel ($E = 200GPa$ and $\upsilon = 0.3$) with a uniform rectangular cross section of $b \times h$ in which $b = 2\ cm$ and $h = 0.5\ cm$ are subjected to axial compressive force as shown in Fig. 1.

Fig.4 explains the convergence of the presented FEM algorithm for two C-C and SS-SS boundary conditions, respectively. It can be observed from both convergence plots that the number of 81 elements is enough to achieve reliable results in the post-buckling problem. Accordingly, the number of 81 elements is selected as the appropriate number in next FEM analyses. It can be clarified quantitatively that the load difference between 81 and 161 elements is about 3% in $w_{max} = 0.04\ m$ for both Figs. 6(a) and 6(b).

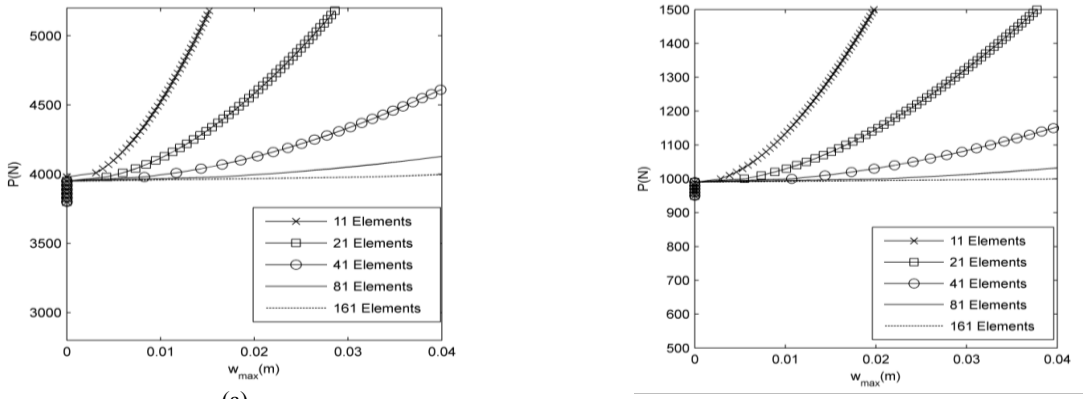

(a) (b)

Fig.4

Convergence of FE method for two boundary conditions and $\frac{a}{h}=0.5$, $\frac{X_0}{L}=0.5$; a) C-C, b) SS-SS.

Considerable difference between formulations and nonlinear results of two analytical and FEM leads to the use of the empirical study to validate. Experimental samples with mentioned geometric and material properties are shown in Fig. 5(a) in which the initial cracks were made in two depths $\frac{a}{h}=0.3$ and , $\frac{a}{h}=0.5$ by using the wire cutting machine. Results of the experimental test are reported based on the buckling test machine as shown in Fig. 5(b).

(a) (b)

Fig.5

a) Experimental samples; b) Buckling test machine.

Fig. 6 shows a comparison between the results of three analytical, FEM and experimental methods. As shown in Fig. 6, FEM and experimental results have a close accordance, while a substantial disagreement with the analytical method is observed in the post-buckling path. However, results of the three methods in the pre-buckling path are remarkably close to each other. The main reason of the error in the nonlinear part of the analytical method is the use of a predefined function Eq. (6) mentioned in [20, 31, 33, 34], to solve the governing differential equation, which is a significant restriction in tracing the post-buckling path. In the other hand, in the nonlinear finite element method, an iterative incremental solution is implemented to determine the deflection at each load level. Therefore, the secant and tangent stiffness matrices are updated at each stage of loading, which leads to the determination of more realistic and precise post-buckling path. Fig. 6 shows that the post-buckling path in the analytical solution rises dramatically after the bifurcation point, while FEM presents a smooth trend. Results of the analytical method represented in Fig. 6(c) are obtained by solving Eqs. (7a) and (7b) in which values of K_c for SS-SS and C-C boundary conditions are calculated 4.9445 and 9.8894, respectively. The deflection pattern is depicted by the determination of relevant coefficients A_i according to Eqs.(C.1) and (C.2) mentioned in Appendix C.

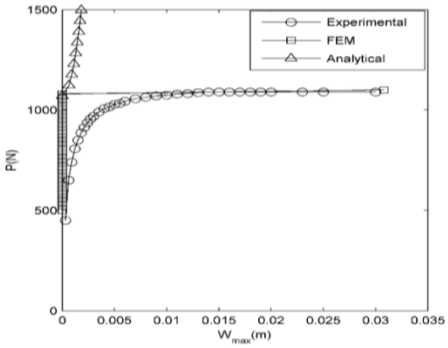

(a)

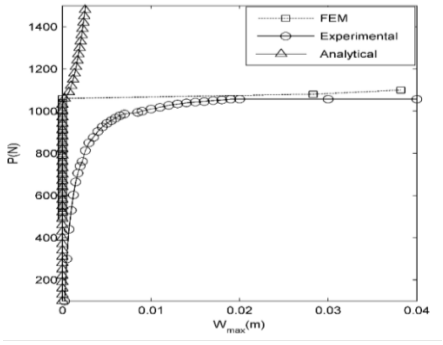

(b)

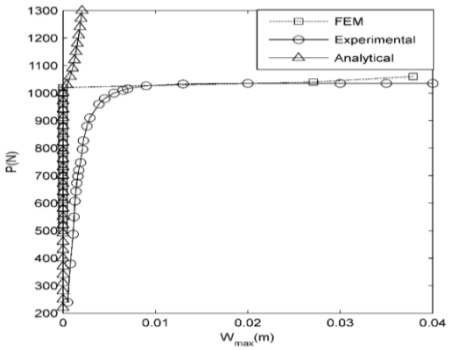

(c)

Fig.6
Validation of the analytical and FE methods through experimental results. a) intact column; b) cracked column with $\frac{a}{h}=0.3$, $\frac{X_0}{L}=0.5$; c) cracked column with $\frac{a}{h}=0.5$, $\frac{X_0}{L}=0.5$ in SS-SS boundary conditions.

Figs. 7(a) and 7(b) depict the critical buckling load and the post-buckling behavior of intact and cracked columns in different crack depths for S-S and C-C boundary conditions, respectively. It is clear from Fig. 7(a) that increasing the cracked depth ratio from 0.3 to 0.5 decreases the critical buckling load from 1060 *N* to 1020 *N* (about 3.8%). In the similar analysis for C-C boundary condition as shown in Fig. 7(b), the load bearing capacity of the column decreases due to the initial crack in which about 5% reduction is observed for the cracked column with $\frac{a}{h}=0.5$ in comparison with the intact column from 4280 *N* to 4080 *N*.

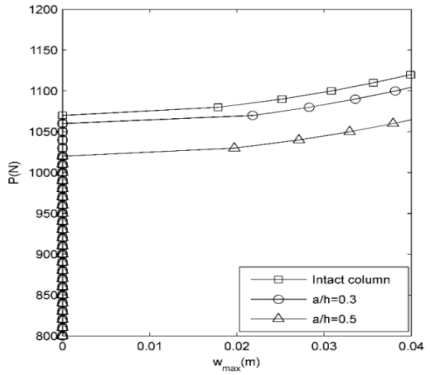

(a)

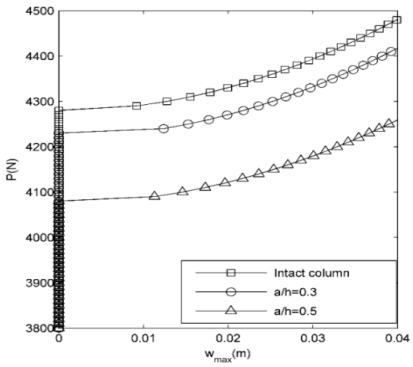

(b)

Fig.7
Post-buckling analysis using FEM in different crack depths and $\frac{X_0}{L}=0.5$. a) S-S; b) C-C boundary conditions.

Fig. 8 illustrates the influence of the crack position on the critical buckling load. Fig. 8(a) for SS-SS boundary condition shows that the minimum critical buckling load is achieved where the crack sits at the middle of the

column. It is also seen from Fig. 8(b) that the maximum critical buckling load for C-C boundary condition belongs to cracked columns that the crack sits at $\frac{X_0}{L} = 0.25$ and 0.75.

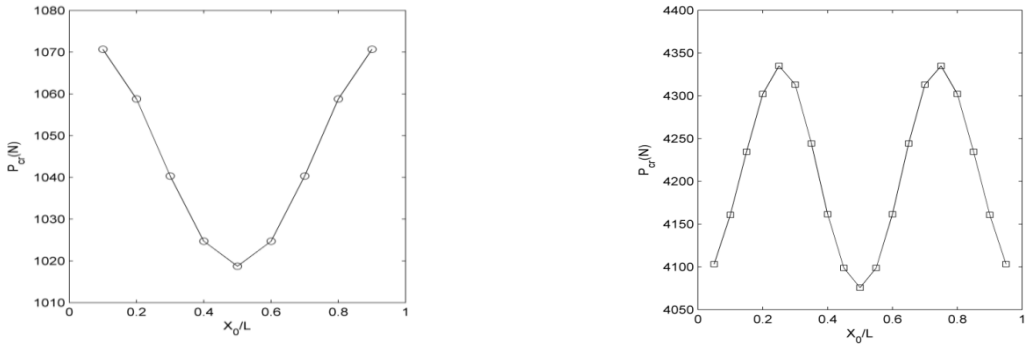

(a) (b)

Fig.8

Critical buckling load of the isotropic column with $\frac{a}{h} = 0.5$ at different crack positions. a) SS-SS; b) C-C.

6 CONCLUSION

The nonlinear buckling analysis of the cracked column was performed by using the three analytical, FE and experimental methods. An in-depth discussion was carried out to investigate results of the common analytical method in analogy with those of experimental and FE methods. A close agreement was shown between results of the empirical tests and FEM, while an obvious difference was seen between the analytical and actual results. A review on the analytical method shows that using a predefined function in the derivation of relations and an iterative solution without updating the structure stiffness are two original reasons in the disagreement of results of the nonlinear part. Since the modification of these two cases in the analytical method is too costly, other reliable methods like FEM are seriously proposed to solve such nonlinear problems. The destructive effect of the crack on the load bearing capacity and the post-buckling path of the cracked column was roughly similar for two SS-SS and C-C boundary conditions.

APPENDIX A

$$
\begin{aligned}
A_4 &= \frac{A_2 L\left(PS_L C_{x0} S_{x0} - PC_L + PC_L C_{x0}^{\,2} + kS_L k_{ds}\right)}{\left(PkS_{x0} C_L\left(x_0 - L\right) + kS_L k_{ds} + PS_L C_{x0} S_{x0} + k^3 EIS_{x0} C_L\left(L - x_0\right) - PC_L + PC_L C_{x0}^{\,2}\right)} \\
A_6 &= -\frac{A_2 x_0 - A_4}{L - x_0} \\
A_7 &= \frac{A_2 L\left(PS_L C_{x0} S_{x0} - PC_L + PC_L^{\,3} + kS_L k_{ds}\right)}{\left(PkS_{x0} C_L\left(x_0 - L\right) + kS_L k_{ds} + PS_L C_{x0} S_{x0} + k^3 EIS_{x0} C_L\left(L - x_0\right) - PC_L + PC_L S_{x0} C_{x0}^{\,2}\right.} \\
A_3 &= -\frac{1}{S_{x0}}\left(-A_4 + A_2 x_0 + A_4 C_{x0} + A_6\left(L - x_0\right) - A_7 S_{x0} + A_7\left(\frac{S_L}{C_L}\right) S_{x0}\right) \\
A_5 &= -A_6 L \\
A_8 &= -A_7\left(\frac{S_L}{C_L}\right) \\
A_1 &= -A_4
\end{aligned}
\qquad \text{(A.1)}
$$

$$
\begin{aligned}
&A_4 = -[A_2(x_0k^2PC_{x0}{}^2 + x_0k^2PS_{x0}{}^2 + x_0k^4EI(C_LS_{x0}{}^2 + C_LC_{x0}{}^2 - S_{x0}{}^2 - C_{x0}{}^2) - Lk^4EIC_L(C_{x0}{}^2 - S_{x0}{}^2) + \\
&k^2PC_L\left(LC_{x0}{}^2 - x_0C_{x0}{}^2 - x_0S_{x0}{}^2 - LC_{x0} + LS_{x0}{}^2\right) - LkPS_LS_{x0} + k^3EIS_L(C_{x0}{}^2 + S_{x0}{}^2) - \\
&kP(S_L(C_{x0}{}^2 + S_{x0}{}^2) + (S_LC_{x0} - C_LS_{x0} + S_{x0}C_{x0}{}^2)) + PS_L{}^2S_{x0})]/ \\
&[k(k^3EI\left(C_{x0}{}^2 - LS_LS_{x0}{}^2 - LS_LC_{x0}{}^2 + x_0S_LC_{x0}{}^2 - C_LC_{x0}{}^2 + x_0S_LS_{x0}{}^2 - C_LS_{x0}{}^2 + S_{x0}{}^2\right) + \\
&kP(C_LS_{x0}{}^2 - x_0S_LC_{x0}{}^2 - C_L{}^2C_{x0} - x_0S_LS_{x0}{}^2 - C_{x0}{}^2 - S_{x0}{}^2 + LS_LC_{x0} + C_LC_{x0}{}^2) - PC_{x0}S_L{}^2 + PS_LS_{x0})] \\
&A_8 = \frac{(-A_4k^3EI\left(S_{x0}{}^2 + C_{x0}{}^2\right) + A_4kP\left(S_{x0}{}^2 - C_LC_{x0} + C_{x0}{}^2\right) + A_2P(C_LS_{x0} - S_{x0}))}{(-k^3EI\left(S_{x0}{}^2 + C_{x0}{}^2\right) - PS_LS_{x0} + kP(S_{x0}{}^2 - C_LC_{x0} + C_{x0}{}^2))} \qquad \text{(A.2)} \\
&A_6 = A_2C_L + \frac{kC_LC_{x0}}{S_{x0}}(A_8 - A_4) + A_8S_L \\
&A_7 = -\frac{A_2}{k} + \frac{C_{x0}}{S_{x0}}(A_4 - A_8) \\
&A_5 = -A_6L - A_7S_L - A_8C_L \\
&A_3 = -A_2/k \\
&A_1 = -A_4
\end{aligned}
$$

$$
\begin{aligned}
&S_L = sin(kL) \\
&C_L = cos(kL) \\
&S_{x0} = sin(kx_0) \\
&C_{x0} = cos(kx_0)
\end{aligned} \qquad \text{(A.3)}
$$

APPENDIX B

The conversion matrices are derived through the energy approach as follows:

$$U_{crack} = U_L + U_R + U_{spring} \qquad \text{(B.1)}$$

$$\Delta\delta U_{crack} = \Delta\delta U_L + \Delta\delta U_R + \Delta\delta U_{spring} \qquad \text{(B.2)}$$

where the components of $\Delta\delta U_{crack}$ are

$$
\begin{aligned}
&\Delta\delta U_L = \delta\boldsymbol{u}_L{}^T\boldsymbol{k}_{TL}\Delta\boldsymbol{u}_L \\
&\Delta\delta U_R = \delta\boldsymbol{u}_R{}^T\boldsymbol{k}_{TR}\Delta\boldsymbol{u}_R \\
&\Delta\delta U_{spring} = \delta\phi^T k_{ds}\Delta\phi
\end{aligned} \qquad \text{(B.3)}
$$

The separated form of displacements is

$$
\begin{aligned}
&\boldsymbol{u}_L = \boldsymbol{C}_L\boldsymbol{u} \\
&\boldsymbol{u}_R = \boldsymbol{C}_R\boldsymbol{u} \\
&\phi = \boldsymbol{C}_{spring}\boldsymbol{u}
\end{aligned} \qquad \text{(B.4)}
$$

So, Eq. (B.2) yields the tangent stiffness matrix of the cracked element as follows:

$$\Delta\delta U_{crack} = \delta\boldsymbol{u}^T\boldsymbol{C}_L{}^T\boldsymbol{k}_{TL}(\boldsymbol{u})\boldsymbol{C}_L\Delta\boldsymbol{u} + \delta\boldsymbol{u}^T\boldsymbol{C}_R{}^T\boldsymbol{k}_{TR}(\boldsymbol{u})\boldsymbol{C}_R\Delta\boldsymbol{u} + \delta\boldsymbol{u}^T\boldsymbol{C}_{spring}{}^T k_{ds}\boldsymbol{C}_{spring}\Delta\boldsymbol{u} \qquad \text{(B.5)}$$

$$\boldsymbol{K}_{T\,crack} = \boldsymbol{K}_{TL} + \boldsymbol{K}_{TR} + \boldsymbol{K}_{spring} \tag{B.6}$$

In which

$$\begin{aligned}
\boldsymbol{K}_{TL} &= \boldsymbol{C}_{L}{}^{T}\boldsymbol{k}_{TL}\boldsymbol{C}_{L} \\
\boldsymbol{K}_{TR} &= \boldsymbol{C}_{R}{}^{T}\boldsymbol{k}_{TR}\boldsymbol{C}_{R} \\
\boldsymbol{K}_{spring} &= \boldsymbol{C}_{spring}{}^{T}k_{ds}\boldsymbol{C}_{spring}
\end{aligned} \tag{B.7}$$

APPENDIX C

$$\begin{aligned}
A_2 &= 1.667e^{7}\left(-\left(7.642e^{27}+3.903e^{2}+1.918e^{19}P^{2}\right)\left(2.4e^{6}P+2.370e^{9}\right)\right)^{\frac{1}{2}} \\
&\quad \left(2.527e^{9}P-5.777e^{11}\right)/\left(1.274e^{27}+6.505e^{22}P+3.197e^{18}P^{2}\right) \\
A_1 &= -\frac{0.63A_2\left(0.998P+930.997\right)}{\left(2.527P-577.706\right)} \\
A_3 &= \frac{6.750A_2\left(0.998P+930.997\right)}{\left(2.527P-577.706\right)} - 2.668A_2 \\
A_4 &= -A_1 \\
A_5 &= -\frac{1.26A_2\left(0.998P+930.997\right)}{\left(2.527P-577.706\right)} + 0.63A_2 \\
A_6 &= \frac{2A_2\left(0.998P+930.997\right)}{\left(2.527P-577.706\right)} - A_2 \\
A_7 &= \frac{6.754A_2\left(0.998P+930.997\right)}{\left(2.527P-577.706\right)} - 2.66A_2 \\
A_8 &= \frac{0.506A_2\left(0.998P+930.997\right)}{\left(2.527P-577.706\right)} - 0.199A_2
\end{aligned} \tag{C.1}$$

$$\begin{aligned}
A_2 &= 5e^{-9}\left(-\left(1.594e^{50}-3.221e^{4}+2.440e^{44}P^{2}-8.214e^{40}P^{3}+1.037e^{37}P^{4}\right)\left(2e^{5}P+7.899e^{8}\right)\right)^{\frac{1}{2}} \\
&\quad \left(-3.845e^{12}+1.935e^{9}P\right)\left(-2.028e^{12}+6.007e^{8}P\right)/ \\
&\quad \left(5.315e^{49}-1.074e^{47}P+8.133e^{43}P^{2}-2.738e^{40}P^{3}+3.457e^{36}P^{4}\right) \\
A_3 &= -0.103A_2 \\
A_4 &= \frac{-0.103A_2\left(-2.403e^{5}+121.233P\right)}{\left(2231.029-0.661P\right)} \\
A_1 &= -A_4 \\
A_5 &= \frac{1}{38455.390-19.348P}(0.103(-2.390e^{5}A_2+120.901A_2P \\
&\quad + \frac{34403.353A_2\left(-2.403e^{5}+121.233P\right)}{\left(2231.029-0.661P\right)} - \frac{18.231PA_2\left(-2.403e^{5}+121.233P\right)}{\left(2231.029-0.661P\right)}
\end{aligned} \tag{C.2}$$

$$A_6 = 0.989A_2 - \frac{13.215A_2\left(-2.403e^5 + 121.233P\right)}{\left(2231.029 - 0.661P\right)} -$$
$$\left(\frac{1}{-38455.3899 + 19.348P}\right)\left(\begin{array}{l} 128.813\left(\frac{1}{\left(223.029 - 0.661P\right)}\right) \\ \left(3949.733A_2\left(-2.403e^5 + 121.233P\right)\right) - \\ 0.00083A_2P - \frac{1.986PA_2\left(-2.403e^5 + 121.233P\right)}{\left(2231.029 - 0.661P\right)} \end{array}\right)$$

$$A_7 = -0.103A_2 + \frac{1.373A_2\left(-2.403e^5 + 121.233P\right)}{\left(2231.029 - 0.661P\right)} +$$
$$\left(\frac{1}{-38455.3899 + 19.348P}\right)\left(\begin{array}{l} 13.364\left(\frac{1}{\left(223.029 - 0.661P\right)}\right) \\ \left(3949.733A_2\left(-2.403e^5 + 121.233P\right)\right) - \\ 0.00083A_2P - \frac{1.986PA_2\left(-2.403e^5 + 121.233P\right)}{\left(2231.029 - 0.661P\right)} \end{array}\right)$$

$$A_8 = \left(\frac{1}{-38455.3899 + 19.348P}\right)\left(\frac{1}{\left(223.029 - 0.661P\right)}\right)\left(3949.733A_2\left(-2.403e^5 + 121.233P\right)\right) -$$
$$0.00083A_2P - \frac{1.986PA_2\left(-2.403e^5 + 121.233P\right)}{\left(2231.029 - 0.661P\right)}$$

REFERENCES

[1] Irwin G.R., 1957, Analysis of stresses and strains near the end of a crack traversing a plate, *Journal of Applied Mechanics* **24**: 361-364.

[2] Alijani A., Abadi M.M., Darvizeh A., Abadi M.K., 2018, Theoretical approaches for bending analysis of founded Euler–Bernoulli cracked beams, *Archive of Applied Mechanics* **88**(6): 875-895.

[3] Ricci P., Viola E., 2006, Stress intensity factors for cracked T-sections and dynamic behaviour of T-beams, *Engineering Fracture Mechanics* **73**(1): 91-111.

[4] Yokoyama T., Chen M.C., 1998, Vibration analysis of edge-cracked beams using a line-spring model, *Engineering Fracture Mechanics* **59**(3): 403-409.

[5] Okamura H., Liu H.W., Chu C.S., Liebowitz H., 1969, A cracked column under compression, *Engineering Fracture Mechanics* **1**(3): 547-564.

[6] Skrinar M., 2019, On the application of the simplified crack model in the bending, free vibration and buckling analysis of beams with linear variation of widths, *Periodica Polytechnica Civil Engineering* **63**(2): 423-431.

[7] Biondi B., Caddemi S., 2005, Closed form solutions of Euler–Bernoulli beams with singularities, *International Journal of Solids and Structures* **42**(9-10): 3027-3044.

[8] Biondi B., Caddemi S., 2007, Euler–Bernoulli beams with multiple singularities in the flexural stiffness, *European Journal of Mechanics-A/Solids* **26**(5): 789-809.

[9] Al-Shayea N.AR., Baluch M.H., Azad A.K., 1987, Influence of non-propagating cracks on conservative buckling of columns, *Transactions of the Canadian Society for Mechanical Engineering* **11**(4): 215-220.

[10] Alijani A., Abadi M.K., Razzaghi J., Jamali A., 2019, Numerical analysis of natural frequency and stress intensity factor in Euler–Bernoulli cracked beam, *Acta Mechanica* **230**(12): 4391-4415.

[11] Mottaghian F., Darvizeh A., Alijani A., 2018, Extended finite element method for statics and vibration analyses on cracked bars and beams, *Journal of Solid Mechanics* **10**(4): 902-928.

[12] Khoei A.R., 2014, *Extended Finite Element Method: Theory and Applications*, John Wiley & Sons.

[13] Rabczuk T., Bordas S.P.A., Askes H., 2010, *Meshfree Discretization Methods for Solid Mechanics*, in Encyclopedia of Aerospace Engineering, Chichester, UK, John Wiley & Sons.

[14] Shirazizadeh M.R., Shahverdi H., 2015, An extended finite element model for structural analysis of cracked beam-columns with arbitrary cross-section, *International Journal of Mechanical Sciences* **99**: 1-9.

[15] Jia L.J., Ge H., 2019, *Ultra-low-Cycle Fatigue Failure of Metal Structures Under Strong Earthquakes*, Springer Nature Singapore Pte Ltd.
[16] Turvey G.J., Zhang Y., 2006, A computational and experimental analysis of the buckling, postbuckling and initial failure of pultruded GRP columns, *Computers & Structures* **84**(22-23): 1527-1537.
[17] Debski H., Teter A., Kubiak T., Samborski S., 2016, Local buckling, post-buckling and collapse of thin-walled channel section composite columns subjected to quasi-static compression, *Composite Structures* **136**: 593-601.
[18] Mazaheri H., Rahami H., Kheyroddin A., 2018, Static and dynamic analysis of cracked concrete beams using experimental study and finite element analysis, *Periodica Polytechnica Civil Engineering* **62**(2): 337-345.
[19] Anifantis N., Dimarogonas A., 1984, Post buckling behavior of transverse cracked columns, *Computers & Structures* **18**(2): 351-356.
[20] Anifantis N., Dimarogonas A., 1983, Imperfection post-buckling analysis of cracked columns, *Engineering Fracture Mechanics* **18**(3): 693-702.
[21] Ke L.L., Yang J., Kitipornchai S., Xiang Y., 2009, Flexural vibration and elastic buckling of a cracked Timoshenko beam made of functionally graded materials, *Mechanics of Advanced Materials and Structures* **16**(6): 488-502.
[22] Bouboulas A., Anifantis N., 2016, Three-dimensional finite element modeling for post-buckling analysis of cracked columns, *International Journal of Structural Integrity* **7**(3): 397-411.
[23] Akbaş Ş.D., 2016, Post-buckling analysis of edge cracked columns under axial compression loads, *International Journal of Applied Mechanics* **8**(08): 1650086.
[24] Akbaş Ş.D., 2019, Post-buckling analysis of a fiber reinforced composite beam with crack, *Engineering Fracture Mechanics* **212**: 70-80.
[25] Akbaş Ş.D., 2015, Post-buckling analysis of axially functionally graded three-dimensional beams, *International Journal of Applied Mechanics* **7**(03): 1550047.
[26] Yang G., Bradford M.A., 2015, Thermoelastic buckling and post-buckling of weakened columns, *Structures* **1**: 12-19.
[27] Kamocka M., Mania R.J., 2019, Post-buckling response of FML column with delamination, *Composite Structures* **230**: 111511.
[28] Ke L.L., Yang J., Kitipornchai S., 2009, Postbuckling analysis of edge cracked functionally graded Timoshenko beams under end shortening, *Composite Structures* **90**(2): 152-160.
[29] Shariati M., Majd Sabeti A.M., Gharooni H., 2014, A numerical and experimental study on buckling and post-buckling of cracked plates under axial compression load, *Journal of Computational & Applied Research in Mechanical Engineering* **4**(1): 43-54.
[30] Yang J., Chen Y., 2008, Free vibration and buckling analyses of functionally graded beams with edge cracks, *Composite Structures* **83**(1): 48-60.
[31] Nayfeh A.H., Emam S.A., 2008, Exact solution and stability of postbuckling configurations of beams, *Nonlinear Dynamics* **54**(4): 395-408.
[32] Ma L.S., Lee D.W., 2012, Exact solutions for nonlinear static responses of a shear deformable FGM beam under an in-plane thermal loading, *European Journal of Mechanics-A/Solids* **31**(1): 13-20.
[33] Emam S.A., Nayfeh A.H., 2009, Postbuckling and free vibrations of composite beams, *Composite Structures* **88**(4): 636-642.
[34] Yaghoobi H., Torabi M., 2013, An analytical approach to large amplitude vibration and post-buckling of functionally graded beams rest on non-linear elastic foundation, *Journal of Theoretical and Applied Mechanics* **51**(1): 39-52.
[35] Nasirzadeh R., Behjat B., Kharazi M., 2018, Finite element study on thermal buckling of functionally graded piezoelectric beams considering inverse effects, *Journal of Theoretical and Applied Mechanics* **56**(4): 1097-1108.
[36] Santos H.A.F.A., Gao D.Y., 2012, Canonical dual finite element method for solving post-buckling problems of a large deformation elastic beam, *International Journal of Non-Linear Mechanics* **47**(2): 240-247.
[37] Cai K., Gao D.Y., Qin Q.H., 2014, Postbuckling analysis of a nonlinear beam with axial functionally graded material, *Journal of Engineering Mathematics* **88**(1): 121-136.
[38] Amara K., Bouazza M., Fouad B., 2016, Postbuckling analysis of functionally graded beams using nonlinear model, *Periodica Polytechnica Mechanical Engineering* **60**(2): 121-128.
[39] Correia J.R., Branco F.A., Silva N.M.F., Camotim D., Silvestre N., 2011, First-order, buckling and post-buckling behaviour of GFRP pultruded beams, Part 1: Experimental study, *Computers & Structures* **89**(21-22): 2052-2064.
[40] Ghavanloo E., 2020, Semi-analytical solution for post-buckling analysis of simply-supported multi-stepped columns, *Structures* **27**: 1086-1092.
[41] Gürel M.A., Kisa M., 2005, Buckling of slender prismatic columns with a single edge crack under concentric vertical loads, *Turkish Journal of Engineering and Environmental Sciences* **29**(3): 185-193.
[42] Wood R.D., Schrefler B., 1978, Geometrically non-linear analysis—A correlation of finite element notations, *International Journal for Numerical Methods in Engineering* **12**(4): 635-642.